35th Annual International Conference of the IEEE EMBS
Osaka, Japan, 3 - 7 July, 2013

Evaluation of the Potential of Multi-modal Sensors for Respiratory Motion Prediction and Correlation

Robert Dürichen[1,2], Lucas Davenport[1], Ralf Bruder[1], Tobias Wissel[1,2], Achim Schweikard[1] and Floris Ernst[1]

Abstract— **In modern robotic radiotherapy, precise radiation of moving tumors is possible by tracking external optical surrogates. The surrogates are used to compensate for time delays and to predict internal landmarks using a correlation model. The correlation depends significantly on the surrogate position and breathing characteristics of the patient. In this context, we aim to increase the accuracy and robustness of prediction and correlation models by using a multi-modal sensor setup. Here, we evaluate the correlation coefficient of a strain belt, an acceleration and temperature sensor (air flow) with respect to external optical sensors and one internal landmark in the liver, measured by 3D ultrasound. The focus of this study is the influence of breathing artefacts, like coughing and harrumphing. Evaluating seven subjects, we found a strong decrease of the correlation for all modalities in case of artefacts. The results indicate that no precise motion compensation during these times is possible. Overall, we found that apart from the optical markers, the strain belt and temperature sensor data show the best correlation to external and internal motion.**

I. INTRODUCTION

The compensation of tumor movements is a challenging problem in stereotactic body radiotherapy (SBRT). These movements are mainly caused by breathing and can have an amplitude of up to 5 cm in extreme cases [1]. In recent years, precise irradiation of moving tumors while sparing surrounding critical structures has become more and more feasible due to new technical developments such as dynamically adjusting multileaf collimators [2] or robotic systems like moving patient couches [3] and the CyberKnife® (Accuray Inc., Sunnyvale, CA) [4]. Here, motion compensation is based on the correlation of external optical surrogates, measured by tracking cameras, with internal landmarks, obtained from stereoscopic X-ray imaging [4], [5]. The correlation model is constantly updated to account for changes in respiration and internal motion pattern. By applying this method, real-time motion compensation is possible due to the high sampling rate of the external surrogates. All technical systems mentioned have to compensate for various sources of latencies. In the case of the CyberKnife® Synchrony system, the latency is 115 ms and mainly caused by mechanical limitations, image acquisition and processing time. This systematic error can be reduced by time series prediction of external surrogates.

The correlation between internal and external motion has been shown in several studies [6], [7]. Even though the correlation is high, Ahn *et al.* [6] reported that the correlation between lung and skin motion strongly depends on the patient. Only 88 % of all patients had a correlation coefficient above 0.6. They conclude that the correlation should be studied for each patient before treatment. Furthermore, Yan *et al.* [8] demonstrated that the correlation between external optical markers (OMs) and the internal landmarks depends on the marker positioning, motion dimension and breathing pattern. It can be increased by using multiple markers. Similar results have been reported by Ernst *et al.* [9] using a net of 19 LEDs. Several authors also investigated the correlation of other physiological signals with internal motion. Kubo *et al.* [10] evaluated the potential of temperature sensors, respiration belts and pneumotachography for respiratory gating techniques. Lu *et al.* [11] compared the correlation of spirometry and abdominal height to the internal air content in lungs. Even though both metrics could be used to accurately predict the internal air content, spirometry showed a stronger and more reproducible relationship. This supports the conclusion of Koch *et al.* [7] that the correlation accuracy can be increased by using multiple surrogates including multiple physiologic parameters.

However, the majority of correlation measurements are done while the patients are breathing freely for a short time period. Considering that e.g. a CyberKnife® session can last up to one hour or more, breathing artefacts like coughing, sneezing and harrumphing are most likely to occur.

In recent years, several promising prediction and correlation algorithms have been presented, which belong to the group of "model-free" algorithms. For example, Ernst *et al.* demonstrated how support vector regression can be used for respiratory motion compensation [12]. The advantage of these algorithms is that they do not need a fixed model as e.g. in case of Kalman Filtering and therefore they can easily be adapted to multi-modal sensor inputs.

We want to investigate how multi-modal surrogates combined with "model-free" algorithms can increase the prediction and correlation accuracy for respiratory motion compensation. As a first step, we analyze the correlation coefficient and the time shift of physiological signals with respect to simultaneously measured infrared markers and an internal landmark (ILM) in the liver. We want to estimate which physiological sensor can most likely be used to increase the prediction and correlation accuracy. Here, we use a strain (respiration belt), an acceleration and a temperature (air flow) sensor. We perform a measurement with seven subjects over five minutes and compare regular and irregular breathing segments.

[1] Institute for Robotics and Cognitive Systems, University of Lübeck, 23538 Lübeck, Germany
[2] Graduate School for Computing in Medicine and Life Sciences, University of Lübeck, 23538 Lübeck, Germany
duerichen at rob.uni-luebeck.de

978-1-4577-0216-7/13/$26.00 ©2013 IEEE

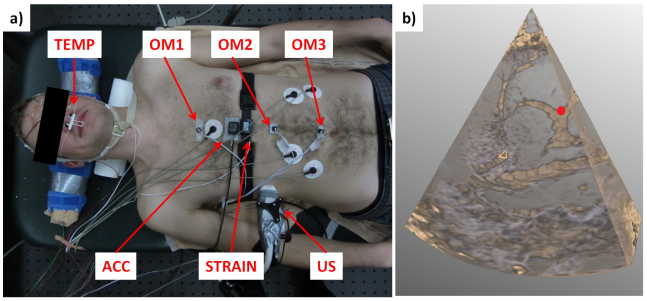

Fig. 1. a) Sensor setup: temperature sensor (TEMP), optical marker 1-3 (OM 1-3), acceleration sensor (ACC), strain sensor (STRAIN) and ultrasound transducer (US). b) Example of an ultrasound image and the selected landmark (red dot).

II. MATERIAL AND METHODS

We performed a multi-modal measurement with seven male test subjects. The sensor setup is shown in fig. 1.a. The signals of three active OMs, one acceleration sensor, a respiration belt, a thermistor and ultrasound of the liver are evaluated. Simultaneously, EMG, EOG and EEG were recorded, but will not be analyzed in this study.
One measurement over five minutes was performed with each subject. Initially, the subjects did breathe freely for two minutes. Afterwards, an acoustic signal was generated 10 times every 15 s. Hearing the signal, they are asked to produce a breathing artefact by coughing, sneezing, harrumphing or speaking.

A. Sensors and synchronzation

Strain and temperature (TEMP): The enlargement of the thorax was measured with a respiration belt and a strain sensor based on piezo-electric crystals (SleepSense®). The respiration belt was placed below the nipples. The respiratory nasal and oral air flow was measured indirectly by a thermistor flow sensor (SleepSense®). These are two commonly available sensors as used in e.g. EEG sleep laboratories. Both signals were directly recorded with a g.tec USB amplifier (g.tec medical engineering GmbH, Austria) at a sampling rate of 1200 Hz.

Position: The position of three OMs was measured with an accuTrack 250 system (Atracsys LLC, Switzerland). The sampling rate was 47 Hz on average and the system has a 3D RMS error of 0.082 mm for moving targets [12]. The OMs are placed along the median line of the thorax and abdomen, starting with OM 1 close to the nipples, OM 2 at the bottom end of the sternum and OM 3 above the navel. The synchronization with the g.tec amplifier was done via strobe values continuously sent from the tracking server. Latencies due to data processing were corrected. The residual maximum latency due to network latencies is below 10 ms.

Acceleration (ACC): One acceleration sensor was placed between OM 1 and the respiration belt. The sensor (STMicroelectronics, LIS3LV02DQ) is a linear accelerator which measures the acceleration of three axes in a range of ± 2 g at a sampling rate of 160 Hz and with a resolution of 12 bit. The synchronization to the amplifier was achieved by a strobe signal of 10 Hz.

Ultrasound (US): We used a modified GE Vivid7 Dimension ultrasound station with a 3V 3D/4D transducer. The frame rate was about 17 Hz. Every recorded frame was synchronized via a strobe signal with the amplifier with a maximum latency of 28 ms [13]. The US probe was attached to the patient couch with a tripod. For each subject, an unambiguous point (e.g. a vessel bifurcation) in the liver was selected as target. In fig. 1.b, a US image example is shown. The selected target is marked by a red dot. The movement of this point had been analyzed before measurement to ensure that it would not leave the field of view of the US probe nor that it would be obscured by the US shadow of the ribs. The targets were tracked in 3D using template matching and sum of squared differences [13]. Template sizes of 15 and 25 pixels^3 and search ranges of 3 and 8 pixels were evaluated, to compensate for unintended jumps of the template in case of strong movements. The best signals were chosen after visual inspection. The spatial resolution is 0.33 mm. We will refer to the target as internal landmark (ILM).

B. Data processing

A 50 Hz filter was applied to the temperature and strain signals. To reduce the dimensionality of the OMs, ILM and ACC, only the first principle component of each signal was used. The principle component of OMs and ACC makes the measurement independent of marker rotations. This reduces the variability of placement errors among subjects. For the correlation of external to external signals, all signals were downsampled and interpolated to the sampling rate of the optical markers and for the correlation of external to internal to the sampling rate of the US data. The correlation coefficient r of a signal x and y is calculated according to Pearson's correlation as

$$r_{x,y}(x,y) = \frac{\sum_{i=1}^{N}(x_i-\bar{x})(y_i-\bar{y}))}{\sqrt{\sum_{i=1}^{N}(x_i-\bar{x})^2\sum_{i=1}^{N}(y_i-\bar{y})^2}}, \qquad (1)$$

where $\bar{x}$ and $\bar{y}$ are the mean of x and y. N is the number of samples available. A correlation coefficient of $r = \pm 1$ means a perfect positive or negative linear correlation of two signals, concluding that the signals are linearly dependent. Two signals are uncorrelated if r is close to zero. Here, we focus on the strength of the correlation and neglect the sign of the correlation coefficient. Therefore only the absolute value is considered. The presented mean and standard deviations of the correlation coefficients are calculated by using the Fisher transform.

III. RESULTS

Fig. 2 shows a typical recording for one subject for a regular (blue line) and irregular (red line) breathing segment. As shown, an artefact strongly influences the amplitude and shape of each signal for all modalities. The shape variations differ depending on the modality. The signal shapes for position and strain are very similar, as the signal of the respiration

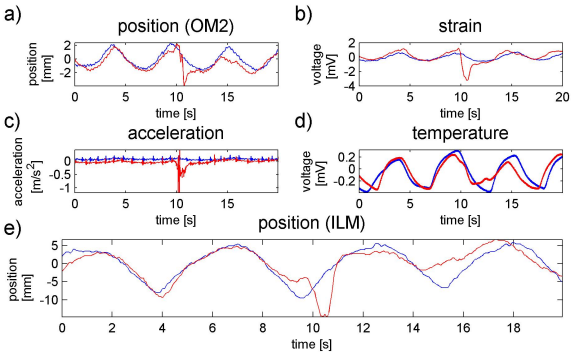

Fig. 2. Typical recordings for one subject of position of OM2 (a), strain (b), acceleration (c), temperature (d) and position of ILM (e) for a regular (blue line) and irregular (red line) breathing segment.

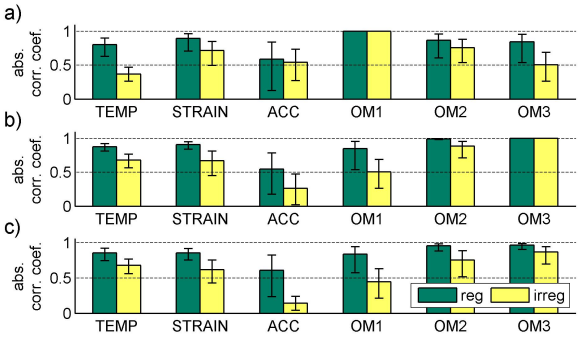

Fig. 3. Mean and standard deviation of the correlation coefficient of temperature, strain, acceleration and position (OM 1-3) with respect to OM1 (a), OM3 (b) and ILM (c) for regular (green) and irregular (yellow) breathing.

belt can be interpreted as the expansion of the complete thorax instead of the position of one point on the thorax. Therefore, the strain signal should be invariant to local rapid movements. The shape of the temperature signal is smoother compared to the other signals. This seems reasonable, taking into account that measuring the temperature difference is an indirect measurement of the air flow and the air flow is a consequence of the thorax movement. Analyzing the acceleration signal in case of an artefact reveals that the highest negative acceleration is shifted in time compared to the minimum peak of the position signal. For comparison Fig. 2.e shows for comparison the position of the ILM.

Fig. 3 shows the mean correlation coefficients and standard deviations for regular and irregular breathing over all subjects. The correlation coefficients are calculated with respect to OM1 (fig. 3.a), the upper marker, OM3 (fig. 3.b), the lower marker and the ILM (fig. 3.c). A time window of $55-115$ s has been chosen for the regular breathing segment, to ignore initial irregular breathing periods. The time window for irregular breathing is $115-260$ s. Due to partially very strong movements of the subjects, the ILM position could not be tracked for all artefacts. These segments have been removed for all sensors. The mean analyzed irregular breathing time is 114.4 s.

To investigate the temporal delay between signals, we shifted the external surrogates with respect to the reference signal by $t_{shift} = \pm 500$ ms in an interval of 10 ms. The correlation coefficient was calculated for each time interval. The mean and standard deviations of the time shifts for the best correlation coefficient is shown in fig. 4 with respect to OM1 (fig. 3.a), OM2 (fig. 3.b) and ILM (fig. 3.c). Comparing fig. 3.a and fig. 3.b reveals that the majority of subjects did chest breathing. OM3 has a mean negative time shift with respect to OM1 and on the other side OM1 has a mean positive time shift with respect to OM3.

IV. DISCUSSION

Evaluating the external correlation of the sensors with each other (fig. 3.a-b) reveals that the position signals have the highest correlation coefficients for both breathing cases. Thereby the correlation decreases with increasing distance between the makers (e.g. fig. 3.a for regular breathing: $r_{OM1,OM1} = 1$, $r_{OM2,OM1} = 0.867$ and $r_{OM3,OM1} = 0.848$). The strain signal has the second highest correlation coefficient. The correlation coefficient for regular breathing is slightly better with respect to OM3 ($r_{str,OM3} = 0.91$) than with respect to OM1 ($r_{str,OM1} = 0.895$), even though the respiration belt lies between OM1 and OM2. The lowest correlation coefficient and the highest standard deviation is featured by the acceleration signal. This was expected, as the acceleration signal is the second derivative of the position signal. Comparing regular and irregular breathing, the correlation coefficients for irregular breathing are lower for all signals and all subjects. For the position signals, the difference between regular and irregular breathing increases with increasing distance between the markers. Similar effects are visible for strain and acceleration signal. Such a comparison is not possible for the temperature signals. The correlation coefficient for the temperature signal is higher with respect to OM3 for both breathing cases ($r_{reg-temp,OM3} = 0.879$ and $r_{irreg-temp,OM3} = 0.681$).

Analyzing the time shift for external correlation (fig. 4.a-b) shows that all surrogates have a high standard deviation. This reveals a big inter-patient variation. The mean absolute time shift of the strain sensor is bigger with respect to OM3 than with respect to OM1 for both breathing cases. These findings are interesting, considering that the respiration belt is placed between OM1 and OM2. Similar results were found for the acceleration signal. The temperature sensor has a negative time shift with respect to OM1. A negative time shift could be expected due to biological and technical time delays, which have not been analyzed further. As the air flow is a consequence of the expansion of thorax and abdomen, these biological time delays cannot be further reduced and depend on the subject and their specific breathing characteristics. The technical time delays are due to the indirect measurement of the flow with a thermistor. These time delays can be reduced by using e.g. a spirometer. However, these sensors are more expensive and more uncomfortable for the patient, if e.g. a mask has to be worn.

Investigating the correlation and time shifts between external

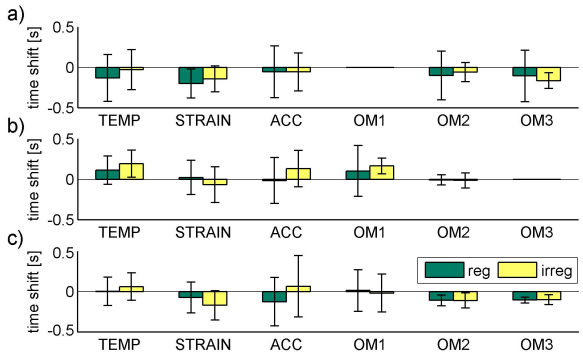

Fig. 4. Mean and standard deviation of the time shift for the best correlation coefficient of temperature, strain, acceleration and position (OM 1-3) with respect to OM1 (a), OM3 (b) and ILM (c) for regular (green) and irregular (yellow) breathing.

and internal signals (fig. 3.c and fig. 4.c) reveals that OM3 has the highest correlation to the position of ILM. Similar as in case of the external correlation with respect to OM3, the correlation of the OMs decreases from OM3 to OM1. For regular breathing the correlation is: $r_{OM3,ILM} = 0.964$, $r_{OM2,ILM} = 0.956$ and $r_{OM1,ILM} = 0.837$. Interestingly, OM3 has a slightly better correlation on average, even though OM2 is the closest marker to the ultrasound transducer (fig. 1.a). For both breathing cases the strain and temperature signals have a higher correlation coefficient than OM3 (e.g. $r_{reg-strain,ILM} = 0.856$, $r_{reg-temp,ILM} = 0.858$). In case of irregular breathing, the mean correlation coefficients decrease for all sensors. Furthermore, the standard deviation increases which indicates that precise motion compensation is difficult. It should be highlighted that the mean correlation of OM1 decreases to $r_{OM1,ILM} = 0.446$. In contrast, the mean correlation of the strain signal decreases only to $r_{strain,ILM} = 0.62$. These findings emphasize that marker placement errors can be reduced by using multi-modal sensor systems. Similar results are visible for the temperature signal. In contrast to the external time shift analysis, the standard deviation of the time shifts for OM2 and OM3 is small. Both mean correlation coefficients are negative for both breathing cases, concluding that the ILM movement occurs earlier compared to the external motion. Going from the abdominal marker OM3 to the chest marker OM1, the mean time shift becomes almost zero.

This study shows that the correlation between external multi-modal surrogates strongly depends on the breathing pattern and artefacts of the subjects. It indicates that during a time period with breathing artefacts no precise motion compensation of tumors is possible and that radiation therapy should be suspended. As illustrated in fig. 2.a and 2.b, the acceleration sensor with its inherent positive time shift to the optical marker position could be used as an indicator of a coming breathing artefact.

In general, the strain and temperature sensors have a high correlation with respect to the OMs and the ILM and, in case of regular breathing, feature a small standard deviation. These modalities have a high potential of increasing the prediction and correlation accuracy in radiation therapy. The temperature sensor could be replaced by a spirometer to increase the correlation and reduce the time shift. Even though the strain sensor is only a one dimensional signal, it measures the expansion of the complete thorax in contrast to the optical markers. A multi-modal correlation algorithm using strain, temperature and optical sensors, should be more robust against improper marker placement.

The study should be extended to a wider and more diverse subject group. Additionally, the subjects should be split into groups, e.g. chest / abdominal breathing or male / female. To further investigate the internal correlation, multiple points in the liver should be considered, including the evaluation rotational effects.

To the authors best knowledge, this was the first correlation study focusing on the comparison between regular and irregular breathing using multi-modal sensors. As a next step, the results of this study will be used in a multi-modal prediction and correlation algorithm.

REFERENCES

[1] P. Giraud, Y. De Rycke, B. Dubray, S. Helfre, D. Voican, L. Guo, J.-C. Rosenwald, K. Keraudy, M. Housset, E. Touboul, and J.-M. Cosset, "Conformal radiotherapy (CRT) planning for lung cancer: analysis of intrathoracic organ motion during extreme phases of breathing," *Int J Radiat Oncol*, vol. 51, no. 4, pp. 1081–1092, 2001.

[2] D. McQuaid and S. Webb, "IMRT delivery to a moving target by dynamic MLC tracking: delivery for targets moving in two dimensions in the beam's eye view," *Phys Med Biol*, vol. 51, no. 19, pp. 4819–4839, 2006.

[3] J. Wilbert, J. Meyer, and K. Baier et. al., "Tumor tracking and motion compensation with an adaptive tumor tracking system (ATTS): system description and prototype testing," *Med Phys*, vol. 35, no. 9, pp. 3911–3921, 2008.

[4] A. Schweikard, G. Glosser, M. Bodduluri, M. J. Murphy, and J. R. Adler, "Robotic motion compensation for respiratory movement during radiosurgery," *Comput Aided Surg*, no. 5, pp. 263–277, 2000.

[5] A. Schweikard, H. Shiomi, and J. Adler, "Respiration tracking in radiosurgery," *Med Phys*, vol. 31, no. 10, pp. 2738–2741, 2004.

[6] S. Ahn, B. Yi, Y. Suh, J. Kim, S. Lee, S. Shin, S. Shin, and E. Choi, "A feasibility study on the prediction of tumour location in the lung from skin motion," *Br J Radiol*, vol. 77, no. 919, pp. 588–596, 2004.

[7] N. Koch, H. Liu, G. Starkschall, M. Jacobson, K. Forster, Z. Liao, R. Komaki, and C. W. Stevens, "Evaluation of internal lung motion for respiratory-gated radiotherapy using MRI: part icorrelating internal lung motion with skin fiducial motion," *Int J Radiat Oncol*, vol. 60, no. 5, pp. 1459–1472, 2004.

[8] H. Yan, F.-F. Yin, G.-P. Zhu, M. Ajlouni, and J. H. Kim, "The correlation evaluation of a tumor tracking system using multiple external markers," *Med Phys*, vol. 33, no. 11, p. 4073, 2006.

[9] F. Ernst, V. Martens, and S. Schlichting et. al., "Correlating chest surface motion to motion of the liver using ε-SVR A porcine study," in *MICCAI*. Springer Berlin Heidelberg, 2009, no. 5762, pp. 356–364.

[10] H. D. Kubo and B. C. Hill, "Respiration gated radiotherapy treatment: a technical study," *Phys Med Biol*, vol. 41, no. 1, pp. 83–91, 1996.

[11] W. Lu, D. A. Low, P. J. Parikh, M. M. Nystrom, I. M. E. Naqa, S. H. Wahab, and M. Handoko et. al., "Comparison of spirometry and abdominal height as four-dimensional computed tomography metrics in lung," *Med Phys*, vol. 32, no. 7, pp. 2351–2357, 2005.

[12] F. Ernst, *Compensating for Quasi-periodic Motion in Robotic Radiosurgery*. Springer US, 2011.

[13] R. Bruder, F. Ernst, A. Schlaefer, and A. Schweikard, "A framework for real-time target tracking in radiosurgery using three-dimensional ultrasound," in *CARS*, vol. 6, 2011, pp. S306–S307.